HHS Public Access

Author manuscript

Acta Biomater. Author manuscript; available in PMC 2018 March 01.

Published in final edited form as:

Acta Biomater. 2017 March 01; 50: 428–436. doi:10.1016/j.actbio.2017.01.010.

One Step Fabrication of Hydrogel Microcapsules with Hollow Core for Assembly and Cultivation of Hepatocyte Spheroids

Christian Siltanen[1,*], **Michaela Diakataou**[1], **Jeremy Lowen**[1], **Amranul Haque**[2], **Ali Rahimian**[1], **Gulnaz Stybayeva**[2], and **Alexander Revzin**[2,*]

[1]Department of Biomedical Engineering, UC Davis, USA

[2]Department of Biomedical Engineering and Physiology, Mayo Clinic, Rochester, MN, USA

Abstract

3D hepatic microtissues can serve as valuable liver analogues for cell-based therapies and for hepatotoxicity screening during preclinical drug development. However, hepatocytes rapidly dedifferentiate *in vitro*, and typically require 3D cultures systems or co-cultures for phenotype rescue. In this work we present a novel microencapsulation strategy, utilizing coaxial flow-focusing droplet microfluidics to fabricate microcapsules with liquid core and poly(ethylene glycol) (PEG) shell. When entrapped inside these capsules, primary hepatocytes rapidly formed cell-cell contacts and assembled into compact spheroids. High levels of hepatic function were maintained inside the capsules for over ten days. The microencapsulation approach described here is compatible with difficult-to-culture primary epithelial cells, allows for tuning gel mechanical properties and diffusivity, and may be used in the future for high density suspension cell cultures.

Graphical abstract

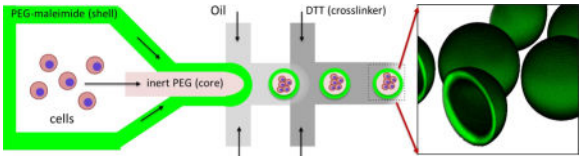

1. Introduction

Hepatic tissue engineering holds great promise for the development of *in vitro* liver toxicity screening platforms,[1] bioartificial liver support devices,[2] and cell-based therapies aimed at treating acute liver failure.[3] However, despite the remarkable regenerative potential of the liver *in vivo*, hepatocytes rapidly dedifferentiate upon isolation from their native microenvironment. In an effort to rescue liver-specific functions *in vitro*, several strategies for recapitulating the hepatic microenvironment have been explored. For example, 3D

Corresponding authors: christian.siltanen@gmail.com, revzin.alexander@mayo.edu.

spheroidal hepatocyte aggregates generated in hanging drops or on non-adhesive substrates exhibit extended metabolic function compared to conventional 2D cultures.[4–7] It has been suggested that enhanced cell-cell contact and the accumulation of autocrine factors, such as epidermal growth factor receptor (EGFR) ligands and deposited ECM, may be at play in enhancing hepatic phenotype in spheroid cultures.[6] Encapsulating spheroids in engineered 3D hydrogels has also been shown to enhance formation of organotypic structures *in vitro*, [8–10] and can improve hepatocyte survival upon transplantation.[11]

Hepatocytes are epithelial cells that require cell-cell contact for survival and function. Therefore, entrapment of hepatocytes in hydrogels typically requires multiple steps, wherein aggregates are first assembled from single cells and are encapsulated only after cell-cell adhesion has been established (typically after 1–2 days).[4, 12, 13] Such multi-step encapsulation approaches are somewhat limited in terms of the throughput and precision of the aggregate formation.

The goal of this study was to develop a facile, one step fabrication process for encapsulation of hepatocytes and formation of hepatic spheroids. In this process, droplet microfluidics were used to *simultaneously* encapsulate a single cell suspension and direct the *self-assembly* of monodisperse organoids in a single step. Droplet microfluidics technologies are capable of encapsulating cells in monodisperse hydrogel particles at remarkable throughput, enabling well controlled high density cultures in a suspension format.[14] Microgels are typically generated by emulsification of a liquid polymer and crosslinked via chemical, ionic, or physical bonding.[15–17] However, controlling the degree of cell-cell contact, a critical parameter for culturing epithelial cells like hepatocytes, can prove challenging when cells are physically entrapped within a hydrogel matrix. Furthermore, decoupling microgel mechanical properties, such as diffusivity and mechanical stiffness (characteristics which may each have independent effects on cell function), is problematic with compositionally uniform materials. In contrast to solid hydrogel particles, core-shell capsules may enable diffusivity to be tuned independently of the core compartment where encapsulated cells reside. Indeed, composite core-shell particles like PLL-coated alginate microgels have been widely explored.[18, 19] Similarly, coaxial flow-focusing droplet microfluidics devices have been used to encapsulate a variety of cell types in hollow core-shell alginate capsules.[20, 21] However, in these reports spheroid formation was driven by proliferation of cells into the capsule lumen. Such capsules may be suboptimal for non-proliferating cells, such as hepatocytes, that require initial contact for survival and subsequent formation of spheroids. In this manuscript, we describe one-step fabrication of liquid-core, hydrogel-shell microcapsules composed of polyethylene glycol (PEG). The liquid core enables single hepatocytes to rapidly find neighbors and form spheroids whereas the hydrogel shell protects cells from shear associated with suspension cultures. To fabricate PEG microcapsules we adapted a protocol for the Michael addition-mediated gelation of maleimide functionalized PEG monomers in the presence of a dithiothrietol (DTT) crosslinker.[16] Encapsulated hepatic spheroids maintained high levels of hepatic phenotype over the course of two weeks. Hepatic function could be enhanced further by culturing encapsulated spheroids atop fibroblast feeder layer. Overall, microcapsules developed here may offer opportunities to develop new suspension cultures or proximal co-culture systems.

2. Materials and Methods

2.1 Fabrication of microfluidic devices

Non-planar flow-focusing devices were fabricated by modifying a previously described protocol.[20] Briefly, top and bottom masters were prepared by spin coating three layers of SU-8 photoresist on a 4-inch silicon wafer. The first layer (60 μm) was exposed to 225 mW-cm^{-2} UV light through a photomask representing the core channel pattern. After a post-exposure bake, the second SU-8 layer (40 μm) was similarly spin coated and exposed through a second photomask corresponding to the shell channel pattern using a mask aligner (ABM, Inc.). This process was repeated for the oil channel layer (50 μm), and then masked regions of photoresist from each layer were chemically etched in a single developing step. Master molds were O_2 plasma cleaned and modified with a fluorinated silane coupling agent, (heptadecafluoro-1,1,2,2-tetrahydrodecyl)dimethylchlorosilane (Gelest), to improve SU-8 durability. PDMS was then poured over masters and replica molded by standard soft lithography procedures. Cured “top” and “bottom” PDMS pieces were then hydroxylated with air plasma (40 seconds) and aligned under a microscope with a thin separating layer of deionized water. Aligned chips were placed on a hotplate at 95°C for 4 h, where bonded devices were then treated with Aquapel solution to render surfaces hydrophobic. The final chip dimensions (height) were a 120 μm core channel, 200 μm shell channel, and 300 μm oil channels (Figure S1).

2.1 Microfluidic device operation and capsule fabrication

Microfluidic coaxial flow-focusing devices were infused with 4 different solutions to generate capsules: 1) a core solution composed of 8% w/v PEG (35 kDa) and 17% Optiprep densifier dissolved in Krebs-Ringer bicarbonate (KRB) buffer, 2) a shell solution containing 4–8% w/v 4-arm maleimide functionalized polyethylene glycol(PEG4MAL) and 10 mM triethanolamine (TEA) dissolved in KRB buffer, 3) a shielding organic phase of mineral oil with 0.5% v/v Span-80 surfactant, and 4) a crosslinking organic phase of mineral oil with 3% Span-80 and a 1:15 emulsion of 25 mg/mL dithiothrietol (DTT) dissolved in DI water (emulsion was generated by sonicating oil/water mixture for 30 min in an ultrasonic bath). Each of the 4 solutions were sterilized with 0.2 μm centrifuge filters, and injected into respective microfluidic inlets with syringe pumps (Harvard Apparatus) at flow rates of 3–5 μL-min^{-1}, 3–5 μL-min^{-1}, 30–50 μL-min^{-1}, and 40–60 μL-min^{-1}, respectively.

2.2 Microcapsule characterization

2.2.1 Fluorescence microscopy—Capsule composition and geometric properties were analyzed by labeling maleimide-functionalized polymers with FITC-PEG-SH or Rhodamine-PEG-SH (Nanocs) (1:1000 PEG to label molar ratio) linkers, and imaged with laser scanning confocal microscopy (Zeiss LSM Pascal).

2.2.2 Dextran diffusion—Diffusive properties of various capsule compositions were visualized by imaging transport of fluorescent dextran polymers across capsule shell barriers. Briefly, capsules were incubated in a solution of 800 μg/mL TRITC-labeled dextran (65–85 kDa) (Sigma) in PBS until saturated, then washed with fresh PBS in a microfluidic

flow chamber and monitored over time with a fluorescence microscope. Average pixel intensities inside capsules (n=5) were quantified in ImageJ.

2.2.3 Rheometry and mesh size analysis—Various conditions of PEG4MAL hydrogel disks were prepared by injecting 90 μL of precursor solutions into 8 mm silicon molds covered with 2000 MWCO dialysis membranes (Sigma). The molds were then immersed in an aqueous solution of 1 mg/mL DTT and incubated overnight to crosslink gels. Storage moduli were measured with a Discovery HR2 hybrid rheometer (TA Instruments) with prefabricated hydrogel disks (n=3) in a parallel-plate geometry, using strain sweep test mode (0–4% strain) and constant oscillating frequency (10 rad-sec^{-1}). A characteristic mesh size, ξ was then estimated following rubber elastic theory (RET) [22] according to Equation 1:

$$\xi = \left(\frac{G' N_A}{RT}\right)^{-1/3} \quad \text{(Eq. 1)}$$

where G′ is the measured storage modulus, N_A is Avogadro's number, R is the universal gas constant, and T is temperature in Kelvin.

2.3 Primary rat hepatocyte isolation

Adult female Lewis rats (125–200 g) were purchased from Charles River Laboratories (Boston, MA) and fed with a commercial diet and water. All animal experiments were performed according to the National Institutes of Health (NIH) guidelines for the ethical care and use of laboratory animals and protocols were approved by the Institutional Animal Care and Use Committee (IACUC) of the University of California, Davis. Primary hepatocytes were isolated using a two-step collagenase perfusion procedure as previously described.[23] Typically, 100–150 million hepatocytes were obtained with viability of 90% or higher as determined by Trypan Blue dye exclusion. For all culture conditions, hepatocytes were maintained in DMEM supplemented with 10% FBS, 200 U/ml penicillin, 200 mg/ml streptomycin, 7.5 mg/ml hydrocortisone sodium succinate, 20 ng/mL epidermal growth factor (EGF), 14 ng/mL glucagon, and 0.5 U/ml recombinant human insulin at 37°C in a humidified 5% CO2 atmosphere. Medium was changed every 24–48 h.

2.4 Hepatocyte encapsulation and culture

For hepatocyte encapsulation experiments, freshly isolated cells were suspended in the core solution at a concentration of 20–40 (10^6) cells-mL^{-1} (which corresponds to 75–150 cells per capsule), and emulsified cell-laden capsules were collected in media on ice. The oil/media mixture was then warmed in a 37°C incubator and gently rocked for 20 minutes, which destabilized emulsions and allowed capsules to sediment down into the aqueous media. Capsules were then collected and copiously washed with fresh media on a 200 μm cell strainer to remove excess oil/DTT, then transferred to 12-well Netwell plates (corning) (~10^5 cells per well) and cultured on a rocker operating at 15 rpm. For unencapsulated spheroid control experiments, freshly isolated hepatocytes were seeded into commercially available Aggrewell 400 plates (Stem Cell) at a density of ~6(10^4) cells-cm^{-2} (~100 cells

per microwell). For 2D monolayer control experiments, hepatocytes were seeded onto type 1 collagen on tissue culture polystyrene at a density of ~1.3(10^5) cells-cm^{-2}. Co-cultures were generated using 3T3-J2 fibroblasts (Kerafast).

2.5 Analysis of hepatic function

Hepatocyte function was assessed by ELISA (Bethyl labs) to measure secreted albumin and by a colorimetric assay (Quantichrom) to measure urea production. For these assays, cell culture supernatant was collected with each media change (n=3) and assayed according to manufacturer instructions. For intracellular immunostaining, spheroids were fixed in 4% paraformaldehyde, embedded in agarose and paraffin, and then sectioned. 5 μm sections were mounted and deparaffinized, then boiled in citrate buffer (pH 6.0) for 40 min for antigen retrieval. Cells were then permeabilized with 0.2% Triton X-100, blocked with 2% BSA for 2h, and incubated with sheep anti-rat albumin primary antibodies (Bethyl labs) overnight at 4°C. Samples were then incubated with Alexafluor 488-conjugated secondary donkey anti-sheep antibodies (Molecular Probes) and 5 ng/mL DAPI for 1.5 h at RT, then imaged with a Nikon Eclipse inverted fluorescence microscope. For hepatic gene expression analysis, total RNA was extracted and purified from encapsulated cells using an RNeasy Plant Mini Kit (Qiagen) per manufacturer instructions. cDNA was synthesized with a Quantitest Reverse Transcription Kit (Roche), and quantitative real-time RT-PCR was performed with universal SYBR Green Master (Roche) in a StepOne qPCR instrument (Thermo Fisher). Relative gene expression was calculated using the comparative threshold cycle (C_t) method with glyceraldehyde 3-phophate dehydrogenase (GAPDH) as a housekeeping gene. qPCR reactions were performed with the following primers in biological triplicate (n=3). Cytochrome P450 3A4(CYP3A4) enzyme activity was evaluated with a P450-Glo CYP3A4 luminescence assay (Promega). Hepatocytes were induced with 50 μM dexamethasone or DMSO control for 48h, then challenged with 50 μM Luciferin-PFBE for 4h. At this point CYP3A4-dependant conversion of Luciferin-PFBE to luciferin was evaluated by measuring luciferase-induced luminescence in an optical plate reader per manufacturer instructions.

2.6 Statistical analysis

Data are represented as mean ± SD. Statistical significance between experimental groups was assessed using a two-tailed student's *t*-tests with Graph Pad 6.0 software, where results were considered statistically significant when p-values were less than *0.05 or *0.01.

3. Results

3.1 Microcapsule fabrication with flow-focusing microfluidics

The microfluidic fabrication of PEG4MAL core-shell microcapsules is schematically illustrated in Figure 1. We used a multilayered PDMS flow-focusing device (Figure S1) to break up a coaxial flow of miscible liquid polymers into discrete core-shell patterned emulsions in an oil carrier phase.[20] The aqueous coaxial flow consisted of an inert, viscous core enclosed in a crosslinkable sheath containing a PEG4MAL solution. At the flow focusing junction, the coaxial stream was emulsified in a "shielding" mineral oil to generate liquid capsule templates, and subsequently introduced to a second oil phase

containing the small molecule crosslinker, DTT, where rapid partitioning of DTT into the aqueous droplets resulted in gelation of the PEG4MAL shell.[16] Hydrogel shell thickness could be modulated by adjusting relative flow rates between core and shell polymer solutions. Figure 2 illustrates the effects of varying core-to-shell flow rate ratios from 1:1 to 1:4 (keeping the core flow constant at 4 μL/min), generating 400 μm capsules with a shell thickness of 10–50 μm. During optimization experiments, we found thinner capsule shells reduced cell entrapment at the core-shell interface. However, further reducing shell thickness below ~10 μm resulted in mechanically unstable capsules. In order to generate microcapsules with the desired core-shell morphology, it was critical to control fluid displacement of the miscible polymer solutions during droplet formation and crosslinking.[24] We found that tuning polymer solution viscosity and the timing of DTT presentation enabled minimal core-shell mixing while still allowing droplet capsules to relax toward a spherical shape with a uniform shell thickness. To modulate the rate of core-shell mixing, we added inert 35 kDa PEG at 0–20% w/v to the core channel. We found that relatively inviscid solutions (<5% w/v PEG) lead to excessive core-shell mixing, while high viscosity solutions (>15% w/v PEG) lead to non-spherical and non-uniform capsule morphology. We therefore used an optimized PEG concentration of 8% w/v for all subsequent experiments. We similarly tested the effects of DTT delivery rate on capsule morphology by adjusting channel geometry and relative flow rates of shielding-to-crosslinking oil phases (varied from 1:2 to 2:1). Again, we observed a tradeoff between excessive core-shell mixing and capsule uniformity as DTT delivery (and therefore crosslinking speed) was decreased or increased, respectively. We thus converged on optimized flow conditions of 1:1 flow rate (40 μL/min each) and a short separating channel (300 μm) between shielding and crosslinking oil phases (Figure 1).

3.2 Mechanical and diffusive properties of PEG4MAL hydrogel shell

Figure 3a–b illustrates the release profiles of 75 kDa rhodamine-dextran from capsules of different hydrogel composition. Despite similar capsule morphology, the ‘half life’ ($t^{1/2}$) of encapsulated dextran increased ~2-fold for the condition of 4% w/v 10 kDa PEG4MAL and 4% w/v 5 kDa PEG4MAL, compared to the more diffusive condition of 4% w/v 10 kDa PEG4MAL alone. Using rubber elastic theory, we estimated a characteristic mesh length in various PEG4MAL hydrogels from their measured storage modulus (Figure 3c).[22] By adjusting the concentration of 10 kDa PEG4MAL from 4% to 8% w/v, we calculated a reduction in pore size from ~14 to 10 nm, respectively. The addition of 2 % w/v 5 kDa PEG4MAL crosslinkers had a more pronounced effect on porosity where average pore size was further reduced to ~7nm.

3.3 Primary hepatocyte encapsulation and culture

Upon encapsulation, we calculated ~83% post-processing viability of PRH cells (normalized to cells stored in cold buffer) by a Trypan blue exclusion assay. After transferring cell-laden capsules to culture media, hepatocytes self-assembled into compact 3D spheroids over the course of 24–48h (Figure 4a). Previous reports have demonstrated that PRH spheroid size plays a significant role in expression of hepatic markers, with aggregates on the order of ~100 μm exhibiting the highest degree of liver-specific functions.[4, 5, 25] With this target aggregate size in mind, we found that loading ~100 cells per capsule generated a PRH

spheroid distribution in the range of 115 ± 10 μm in diameter. When compared to seeding in a commercially available micropatterned culture plate (Aggrewell 400™, StemCell Technologies), we found our encapsulation method to generate spheroids with slightly improved uniformity and circularity (Figure 4b–c). The increased polydispersity among unencapsulated spheroids may be due to errors in evenly plating cells by hand. We maintained encapsulated hepatospheres in continuously stirred suspension culture for the remaining experiments, and compared hepatic function to cells cultured in static conditions in Aggrewell plates or in monolayers on collagen. We found that spheroids in suspension culture synthesized increased levels of albumin and urea (Figure 5a–b) compared to controls, and stained positively for intracellular albumin(Figure 5c–d). These data suggest gas/nutrient transport may play an important role in hepatocyte functional maintenance. Although culturing unencapsulated spheroids on a rocking plate also led to increased albumin production at early time points (data not shown), this condition resulted in excessive merging of individual spheroids into macroscopic aggregates. qRT-PCR analysis similarly revealed that spheroids in suspension significantly upregulated albumin and liver-specific enzyme gene expression, including glucose 6-phosphotase (G6Pase) and tyrosine aminotransferase (TAT) (Figure 6).

3.4 Co-culture with 3T3-J2 fibroblasts

As shown in Figure 7a–b, encapsulated PRH spheroids increased albumin synthesis when co-cultured atop a layer of 3T3 fibroblasts. Similarly, CYP3A4 enzyme activity, a cytochrome P450 family member responsible for the metabolism of dexamethasone, was increased ~1.5-fold in response to dexamethasone induction in co-culture conditions (Figure 7c), whereas increases over basal level were negligible under monoculture conditions. To test the effects of proximity between cell types on hepatic function, we repeated co-culture experiments with capsules either seeded directly atop a fibroblast monolayer, or separated by 1mm using a transwell culture plate (Figure 7D). We found that separating the two cell types abrogated the effects of co-culture on albumin secretion, perhaps indicating a role of transport limited cell-cell communication *via* soluble growth factors.

4. Discussion

Cell encapsulation is a promising route for both the development of improved transplantation delivery vehicles and large scale suspension culture of anchorage-dependent cells and tissues. One of the key benefits of microencapsulation is the ability to protect cells from fluidic shear stress while ensuring rapid transport provided by stirred or perfused culture environments.[26] For example, hepatic spheroids have been shown to benefit from perfusion in microfluidic devices, but suffer loss of function under hydrodynamic shear stress.[27] For cell encapsulation applications, it is important to control transport between encapsulated cells and the external environment, for example to provide immunoisolation[26], retain and accumulate cell-secreted soluble factors,[28] or ensure adequate exchange of gases, nutrients, and waste. To demonstrate how microcapsule diffusivity can be tuned by varying PEG4MAL composition, we performed rheological and transport analyses on several hydrogel conditions used for microcapsule fabrication. These mesh size calculations suggest that even large serum proteins (e.g. albumin (R_H = 3.56 nm)

[29] can be exchanged across the capsule shell in all tested conditions, albeit at a tunable but limited rate. While we cannot expect this rheological mesh analysis performed on *macroscopic* gels to precisely reflect the mechanical properties of *microfabricated* capsules, these results demonstrate how our PEG-based biomaterial affords significant flexibility in terms of protein diffusivity, which may be useful in applications where selective capsule permeability is desirable (e.g. immunoisolation or accumulation of autocrine factors). The biocompatibility of the flow-focusing reagents and mild crosslinking chemistry of PEG4MAL was exemplified by the microencapsulation of primary rat hepatocytes (PRH), which are notoriously sensitive to fluidic shear stress and excessive processing.[2] Although we reported a ~17% loss in viability due to processing, these cells were capable of forming functional spheroids comparable to unprocessed controls. Crosslinking of microgels was accomplished with a radical-free, bioorthogonal coupling of PEG4MAL with the small molecule DTT. The maleimide functional groups were chosen for their high specificity and rapid reaction kinetics with free sulfhydryls under physiologic conditions via a nucleophilic Michael addition reaction.[30] It is important to note that PRH self-assembly was highly dependent on a well-defined boundary at the core-shell interface, where a thicker or less uniform hydrogel shell morphology resulted in excessive cell entrapment at the interface, leading to poor spheroid assembly. This finding is in line with our previous reports of poor hepatocyte viability when encapsulated in PEG hydrogels as single cells.[31] One limitation of our current PEG encapsulation scheme is the inability to easily degrade the hydrogel for intact cell retrieval. However, several research groups have developed robust methods for integrating hydrolytically labile, protease cleavable, or photodegradable linkers into PEG hydrogels,[32–34] which could offer new capabilities to our system.

Several in vitro studies have shown that cultured hepatocytes can benefit from heterotypic interactions with nonparenchymal cells that secrete inductive growth factors and/or ECM proteins.[35–37] Bhatia and colleagues have shown that murine 3T3 fibroblasts induce hepatic albumin secretion when cultured in close proximity to clustered hepatocyte islands on micropatterned surfaces. [38] However, collecting purified hepatocytes from these co-cultures for downstream analysis or application can be somewhat challenging. In contrast, microencapsulated hepatic spheroids can be cultured directly atop a 3T3 fibroblast monolayer without mixing of the two cell types. In this format hepatocytes were kept with ~10 μm of fibroblasts (determined by the thickness of the PEG hydrogel shell), yet hydrogel microcapsules did not adhere to the feeder layer and could be easily collected for further cultivation or downstream analysis.

5. Conclusions

While encapsulation of cells in hydrogels is widely practiced by the bioengineering community, challenges in the field remain. This is particularly true when it comes to entrapment of slow proliferating cells that require cell-cell contact for survival and function. For hepatocytes, this challenge is typically addressed with a multi-step process where cells are first formed into aggregates and then encapsulated.[39, 40] Herein, we describe an alternative one step strategy combining capsule fabrication, hepatocyte encapsulation and cell aggregate formation. Microfluidic devices with coaxial flow focusing were used to create polymer droplets, composed of cross-linkable PEG4Mal and inert PEG, in mineral

oil. On-chip reaction with thiol-containing cross-linker (DTT) resulted in gelation of the shell. After emulsion was broken up, the inert PEG in the core of a droplet leeched out, creating a composite liquid core/hydrogel shell microcapsule. Importantly, the process of emulsification and gelation was compatible with primary hepatocytes. These cells were introduced along with PEG into the microfluidic device, survived encapsulation, formed spheroids in the liquid core and remained functional for two weeks in culture. Importantly, hepatic function was maintained at levels that were comparable to or better than standard unencapsulated hepatic spheroids. Furthermore, microcapsules with entrapped hepatocytes could be cultured atop a fibroblast feeder layer to further enhance hepatic function. In this co-culture method hepatocyte spheroids were separated from the feeder cells by a thickness of hydrogel shell ~10 μm. Importantly, microcapsules gently rested atop fibroblast layer but did not adhere and could be removed by simple aspiration. The ability to easily de-couple co-cultures and collect the desired cell type may offer interesting opportunities for cell-type specific analysis or continued cultivation of cells. The core-shell microcapsules described here are compatible with on-chip microgel washing/collection procedures described elsewhere,[41, 42] and may hold promise for future use in suspension cultures or bioreactors. In addition, such microcapsules may facilitate multi-step co-culture experiments in the future.

Supplementary Material

Refer to Web version on PubMed Central for supplementary material.

Acknowledgments

The work presented in this paper was supported in part by the NIH grant R0107255.

References

1. Soldatow VY, LeCluyse EL, Griffith LG, Rusyn I. In vitro models for liver toxicity testing. Toxicology research. 2013; 2(1):23–39. [PubMed: 23495363]
2. Allen JW, Hassanein T, Bhatia SN. Advances in bioartificial liver devices. Hepatology. 2001; 34(3): 447–455. [PubMed: 11526528]
3. Gupta JR, Chowdhary S, Chowdhary JR. Hepatocyte transplantation: back to the future. Hepatology. 15(1):0270–9139.
4. Gevaert E, Dollé L, Billiet T, Dubruel P, van Grunsven L, van Apeldoorn A, Cornelissen R. High Throughput Micro-Well Generation of Hepatocyte Micro-Aggregates for Tissue Engineering. PLoS ONE. 2014; 9(8)
5. Brophy CM, Luebke-Wheeler JL, Amiot BP, Khan H, Remmel RP, Rinaldo P, Nyberg SL. Rat hepatocyte spheroids formed by rocked technique maintain differentiated hepatocyte gene expression and function. Hepatology. 2009; 49(2):578–586. [PubMed: 19085959]
6. Williams CM, Mehta G, Peyton SR, Zeiger AS, Vliet KJ, Griffith LG. Autocrine-Controlled Formation and Function of Tissue-Like Aggregates by Primary Hepatocytes in Micropatterned Hydrogel Arrays. Tissue Eng. 2011; Part A 17(7–8):1055–1068.
7. Koide N, Koide Y Sakaguchi K, Asano K Koide Y, Kawaguchi M Asano K, Matsushima H Kawaguchi M, Takenami T Matsushima H, Shinji T Takenami T, Mori M Shinji T, Tsuji T Mori M, Tsuji T. Formation of multicellular spheroids composed of adult rat hepatocytes in dishes with positively charged surfaces and under other nonadherent environments. Exp Cell Res. 1990; 186(2): 227–235. [PubMed: 2298241]

8. Kim M, Lee J, Jones CN, Revzin A, Tae G. Heparin-based hydrogel as a matrix for encapsulation and cultivation of primary hepatocytes. Biomaterials. 2010; 31(13):3596–3603. [PubMed: 20153045]
9. Foster E, You J, Siltanen C, Patel D, Haque A, Anderson L, Revzin A. Heparin hydrogel sandwich cultures of primary hepatocytes. European Polymer Journal. 2015; 72:726–735.
10. Dunn JC, Koebe HG Yarmush Ml, Tompkins RG Koebe Hg, Tompkins RG. Hepatocyte function and extracellular matrix geometry: long-term culture in a sandwich configuration. FASEB J. 1989; 3(2):174–177. [PubMed: 2914628]
11. Jitraruch S, Dhawan A, Hughes RD, Filippi C, Soong D, Philippeos C, Lehec SC, Heaton ND, Longhi MS, Mitry RR. Alginate microencapsulated hepatocytes optimised for transplantation in acute liver failure. PLoS One. 2014; 9(12)
12. Tostoes RM, Leite JP, Miranda M, Sousa DIC, Wang Di MJT, Carrondo PM, Alves PM. Perfusion of 3D encapsulated hepatocytes–a synergistic effect enhancing long-term functionality in bioreactors. Biotechnol Bioeng. 2011; 108(1):41–49. [PubMed: 20812261]
13. Li CY, Stevens RE, Schwartz BS, Alejandro JH, Huang1 SN, Bhatia SN. Micropatterned cell-cell interactions enable functional encapsulation of primary hepatocytes in hydrogel microtissues. Tissue Eng Part A. 2014; 20(15–16):22100–2012.
14. Siltanen C, Yaghoobi M, Haque A, You J, Lowen J, Soleimani M, Revzin A. Microfluidic fabrication of bioactive microgels for rapid formation and enhanced differentiation of stem cell spheroids. Acta Biomaterialia. 2016; 34:125–132. [PubMed: 26774761]
15. Rossow T, Heyman JA, Ehrlicher AJ, Langhoff A, Weitz DA, Haag R, Seiffert S. Controlled Synthesis of Cell-Laden Microgels by Radical-Free Gelation in Droplet Microfluidics. Journal of the American Chemical Society. 2012; 134(10):4983–4989. [PubMed: 22356466]
16. Headen DM, Aubry G, Lu H, García AJ. Microfluidic-Based Generation of Size -Controlled, Biofunctionalized Synthetic Polymer Microgels for Cell Encapsulation. Advanced Materials. 2014; 26(19):3003–3008. [PubMed: 24615922]
17. Hwang YS, Cho F, Tay JYY, Heng R, Ho SG, Kazarian DR, Williams AR, Boccaccini JM, Polak A, Mantalaris A. The use of murine embryonic stem cells, alginate encapsulation, and rotary microgravity bioreactor in bone tissue engineering. Biomaterials. 2009; 30(4):499–507. [PubMed: 18977027]
18. Zhang W, Zhao S, Rao W, Snyder J, Choi JK, Wang J, Khan IA, Saleh NB, Mohler PJ, Yu J, Hund TJ, Tang C, He X. A novel core–shell microcapsule for encapsulation and 3D culture of embryonic stem cells. Journal of Materials Chemistry B. 2012; 1(7):1002–1009.
19. Wang X, Wang W, Ma J, Guo X, Yu X, Ma X. Proliferation and Differentiation of Mouse Embryonic Stem Cells in APA Microcapsule: A Model for Studying the Interaction between Stem Cells and Their Niche. Biotechnology Progress. 2006; 22(3):791–800. [PubMed: 16739963]
20. Agarwal P, Zhao S, Bielecki P, Rao W, Choi J, Zhao Y, Yu J, Zhang W, He X. One-step microfluidic generation of pre-hatching embryo-like core–shell microcapsules for miniaturized 3D culture of pluripotent stem cells. Lab on a Chip. 2013; 13(23):4525–4533. [PubMed: 24113543]
21. Chen Q, Utech S, Chen D, Prodanovic R, Lin JM, Weitz DA. Controlled assembly of heterotypic cells in a core-shell scaffold: organ in a droplet. Lab on a Chip. 2016; 16(8):1346–1349. [PubMed: 26999495]
22. Welzel P, Prokoph S, Zieris A, Grimmer M, Zschoche S, Freudenberg U, Werner C. Modulating Biofunctional starPEG Heparin Hydrogels by Varying Size and Ratio of the Constituents. Polymers. 2011; 3(1)
23. Hepatocytes in collagen sandwich: evidence for transcriptional and translational regulation. The Journal of Cell Biology. 1992; 116(4):1043–1053. [PubMed: 1734019]
24. Huang H, He X. Fluid displacement during droplet formation at microfluidic flow-focusing junctions. Lab on a Chip. 2015; 15(21):4197–4205. [PubMed: 26381220]
25. Glicklis R, Merchuk S, Cohen S. Modeling mass transfer in hepatocyte spheroids via cell viability, spheroid size, and hepatocellular functions. Biotechnol Bioeng 20. 2004; 86(6):672–680.
26. Wilson JL, McDevitt TC. Stem cell microencapsulation for phenotypic control, bioprocessing, and transplantation. Biotechnology and Bioengineering. 2013; 110(3):667–682. [PubMed: 23239279]

27. Tong WH, Fang Y, Yan J, Hong X, Singh N Hari, Wang SR, Nugraha B, Xia L, Fong ELS, Iliescu C, Yu H. Constrained spheroids for prolonged hepatocyte culture. Biomaterials. 2016; 80:106–120. [PubMed: 26708088]

28. Baker BM, Chen CS. Deconstructing the third dimension: how 3D culture microenvironments alter cellular cues. Journal of Cell Science. 2012; 125(Pt 13):3015–3024. [PubMed: 22797912]

29. Weber LM, Lopez CG, Anseth KS. Effects of PEG hydrogel crosslinking density on protein diffusion and encapsulated islet survival and function. Journal of biomedical materials research. 2009; Part A 90(3):720–9.

30. García AJ. PEG–Maleimide Hydrogels for Protein and Cell Delivery in Regenerative Medicine. PEG–Maleimide Hydrogels for Protein and Cell Delivery in Regenerative Medicine. 2014

31. Kim M, Lee JY, Jones CN, Revzin A, Tae G. Heparin-based hydrogel as a matrix for encapsulation and cultivation of primary hepatocytes. Biomaterials. 2010; 31(13):3596–3603. [PubMed: 20153045]

32. Siltanen C, Shin DS, Sutcliffe J, Revzin A. Micropatterned Photodegradable Hydrogels for the Sorting of Microbeads and Cells. Angewandte Chemie International Edition. 2013; 52(35):9224–9228. [PubMed: 23868693]

33. Shin DS, You J, Rahimian A, Vu T, Siltanen C, Ehsanipour A, Stybayeva G, Sutcliffe J, Revzin A. Photodegradable Hydrogels for Capture, Detection, and Release of Live Cells. Angewandte Chemie International Edition. 2014; 53(31):8221–8224. [PubMed: 24931301]

34. Griffin DR, Weaver WM, Scumpia PO, Di Carlo D, Segura T. Accelerated wound healing by injectable microporous gel scaffolds assembled from annealed building blocks. Nat Mater. 2015; 14(7):737–744. [PubMed: 26030305]

35. Bhatia SN, Balis UJ, Yarmush ML, Toner M. Effect of cell-cell interactions in preservation of cellular phenotype: cocultivation of hepatocytes and nonparenchymal cells. FASEB journal: official publication of the Federation of American Societies for Experimental Biology. 1999; 13(14):1883–1900. [PubMed: 10544172]

36. March S, Ramanan V, Trehan K, Ng S, Galstian A, Gural N, Scull MA, Shlomai A, Mota MM, Fleming HE, Khetani SR, Rice CM, Bhatia SN. Micropatterned coculture of primary human hepatocytes and supportive cells for the study of hepatotropic pathogens. Nat Protocols. 2015; 10(12):2027–2053. [PubMed: 26584444]

37. You VK, Raghunathan KJ, Son D, Patel A, Haque CJ, Murphy A, Revzin A. Impact of Nanotopography, Heparin Hydrogel Microstructures, and Encapsulated Fibroblasts on Phenotype of Primary Hepatocytes. ACS Appl Mater Interfaces 17. 2015; 7(23):12299–308.

38. Khetani SR, Bhatia SN. Microscale culture of human liver cells for drug development. Nature Biotechnology. 2007; 26(1):120–126.

39. Albrecht DR, Underhill GH, Wassermann TB, Sah RL, Bhatia SN. Probing the role of multicellular organization in three-dimensional microenvironments. Nat Methods. 2006; 3(5):369–75. [PubMed: 16628207]

40. Li CY, Stevens KR, Schwartz RE, Alejandro BS, Huang JH, Bhatia SN. Micropatterned Cell-Cell Interactions Enable Functional Encapsulation of Primary Hepatocytes in Hydrogel Microtissues. Tissue Eng Part A. 2014; 20(15–16):2200–2212. [PubMed: 24498910]

41. Agarwal P, Choi JK, Huang H, Zhao S, Dumbleton J, Li J, He X. A Biomimetic Core–Shell Platform for Miniaturized 3D Cell and Tissue Engineering.

42. Huang H, He X. Interfacial tension based on-chip extraction of microparticles confined in microfluidic Stokes flows. Applied Physics Letters. 2014; 105(14):143704. [PubMed: 25378709]

Our paper combines an interesting new way for making capsules with cultivation of difficult-to-maintain primary epithelial cells (hepatocytes). The microcapsules described here will enable high density suspension culture of hepatocytes or other cells and may be used as building blocks for tissue engineering applications.

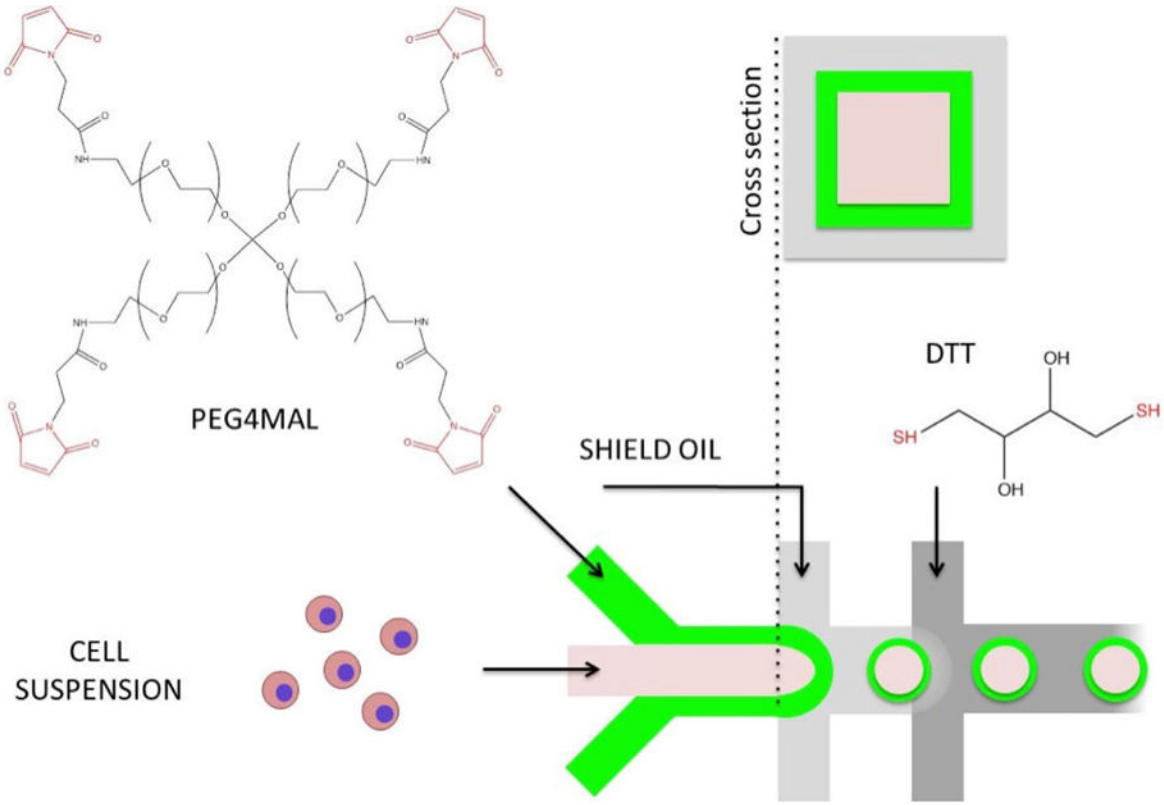

Figure 1. Schematic illustration of microcapsule fabrication process

A) Microfluidic flow-focusing device is infused with two aqueous streams one containing cell suspension, another carrying 4-arm PEG-maleimide (PEG4MAL). These aqueous streams experience minimal mixing due to differences in viscosity. Core-shell particle patterning is achieved by generating coaxial flow (see cross-section) upstream of flow-focusing junction. Emulsification occurs by exposure to two oil streams, the first one designed to stabilize aqueous droplets the second one to deliver a crosslinker DTT to gel PEG4MAL.

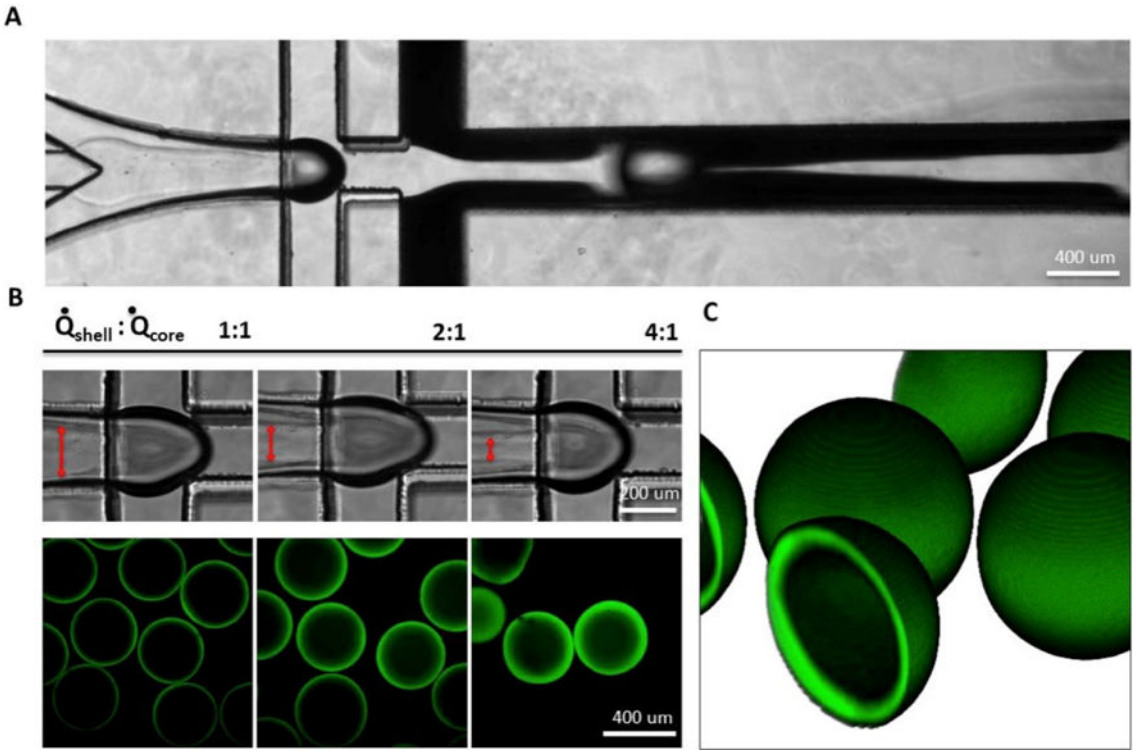

Figure 2. Microcapsule fabrication

A) Coaxial flow-focusing generates hollow core-shell capsules. B) Shell thickness (visualized with FITC-PEG-SH) was varied by modulating core/shell flow rate ratio. C) 3D reconstruction of z-stacked confocal microcapsule images. Capsule diameter is ~400 μm, shell thickness is ~10 μm.

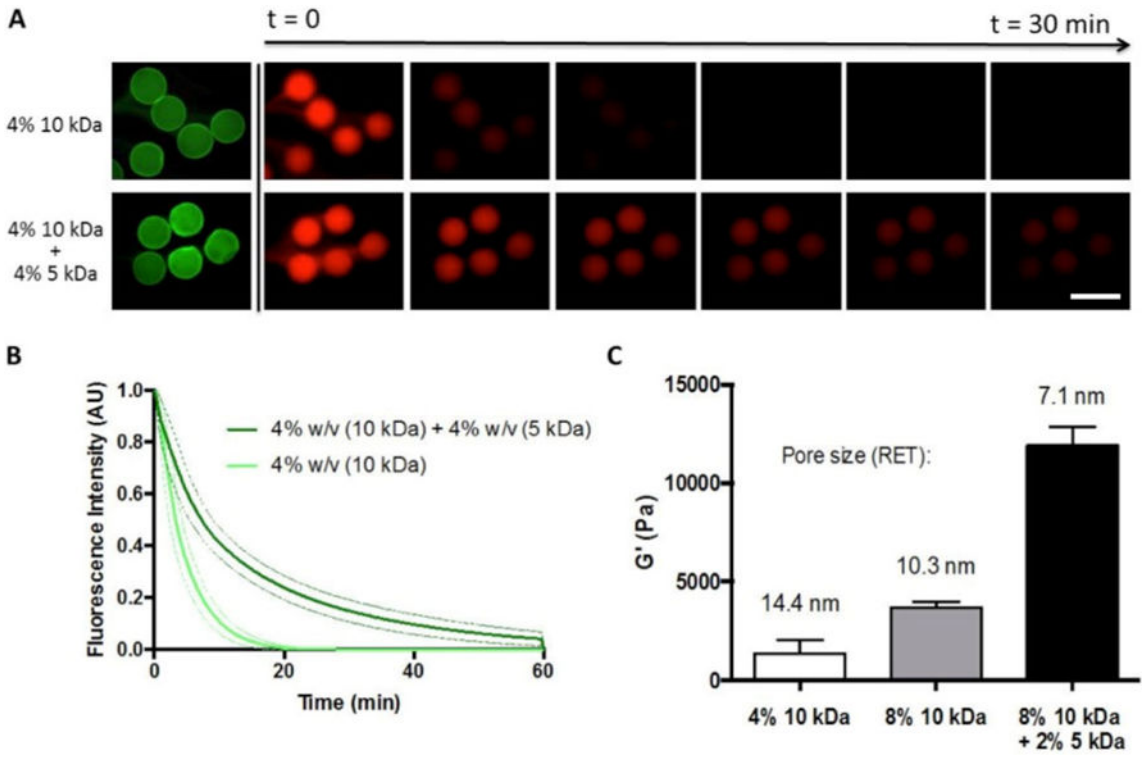

Figure 3. Assessing the effects of PEG4MAL MW and concentration on diffusive properties of hydrogel shell

A) Release of 75kDa rhodamine-dextran (red) from capsules of varying polymer composition. Fluorescein-labeled PEG (green) is used to visualize B) Fluorescence intensity of capsules over time. Dotted lines represent ± 1 SD from measured capsules (n=5). C) Bulk storage modulus was used to estimate a characteristic mesh size for each capsule condition (n=3). Scale bar = 500 μm.

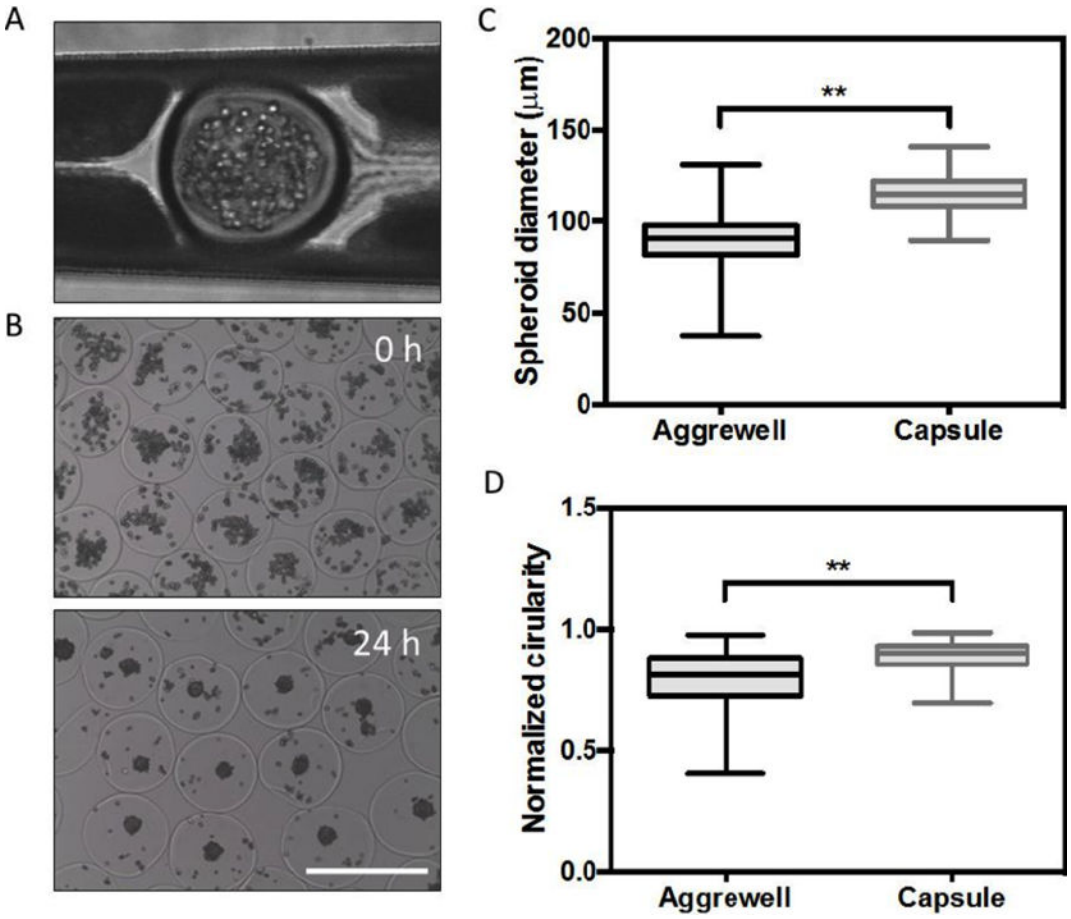

Figure 4. Primary rat hepatocyte encapsulation and spheroid assembly

(A) a cell-laden capsule undergoing DTT-induced crosslinking in a microfluidic device (top). Encapsulated hepatocytes in aqueous media immediately after collection (middle). Aggregated cells assembled into compact spheroids after ~24–48h. (B-C) spheroids generated by encapsulation exhibited greater consistency in terms of size and circularity compared to those generated in Aggrewell™ plates (histograms collected from n=100 representative capsules, * $p<0.05$, ** $p<0.01$). Scale bar = 500 μm.

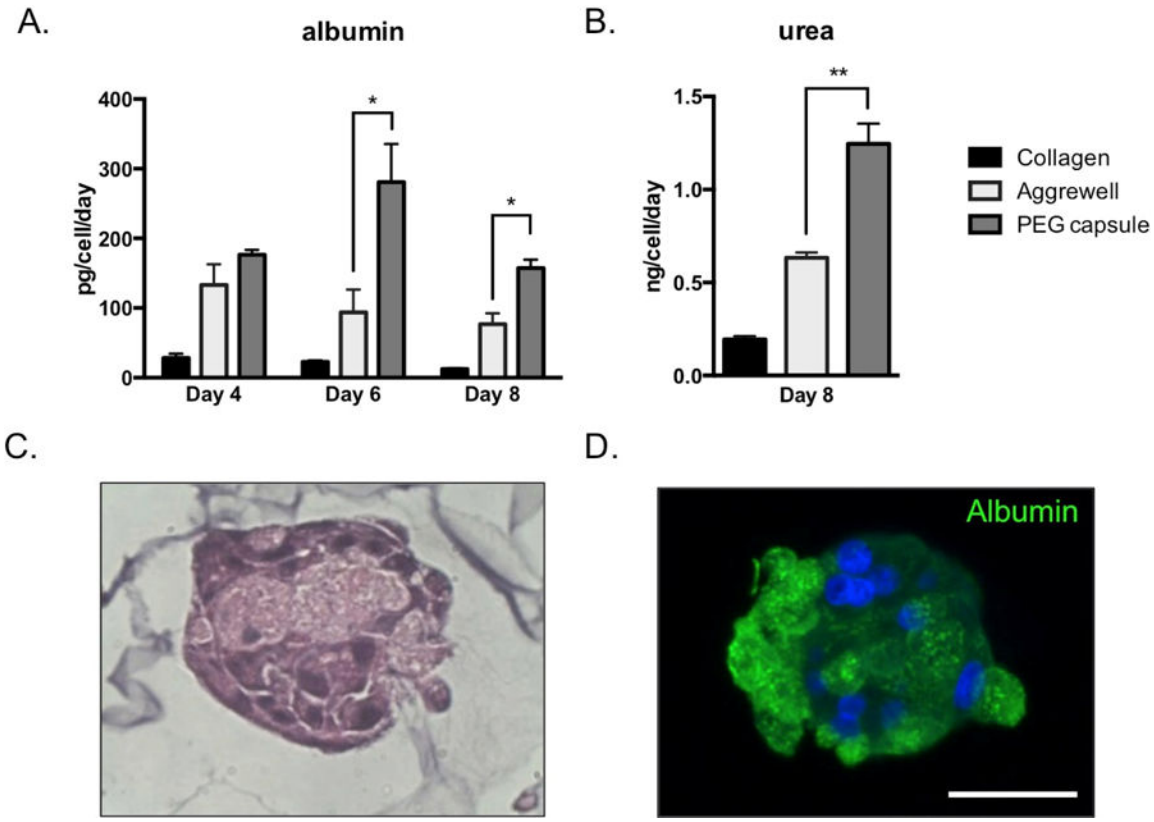

Figure 5. Function of encapsulated hepatocytes

(A–B) ELISA results and colorimetric assays indicate encapsulated spheroids secreted higher levels of albumin and urea, respectively, compared to 2D or 3D controls (n=3). (C-D) H&E histology and immunofluorescence staining indicates intracellular albumin in encapsulated hepatic spheroids (Day 7). * $p<0.05$, ** $p<0.01$

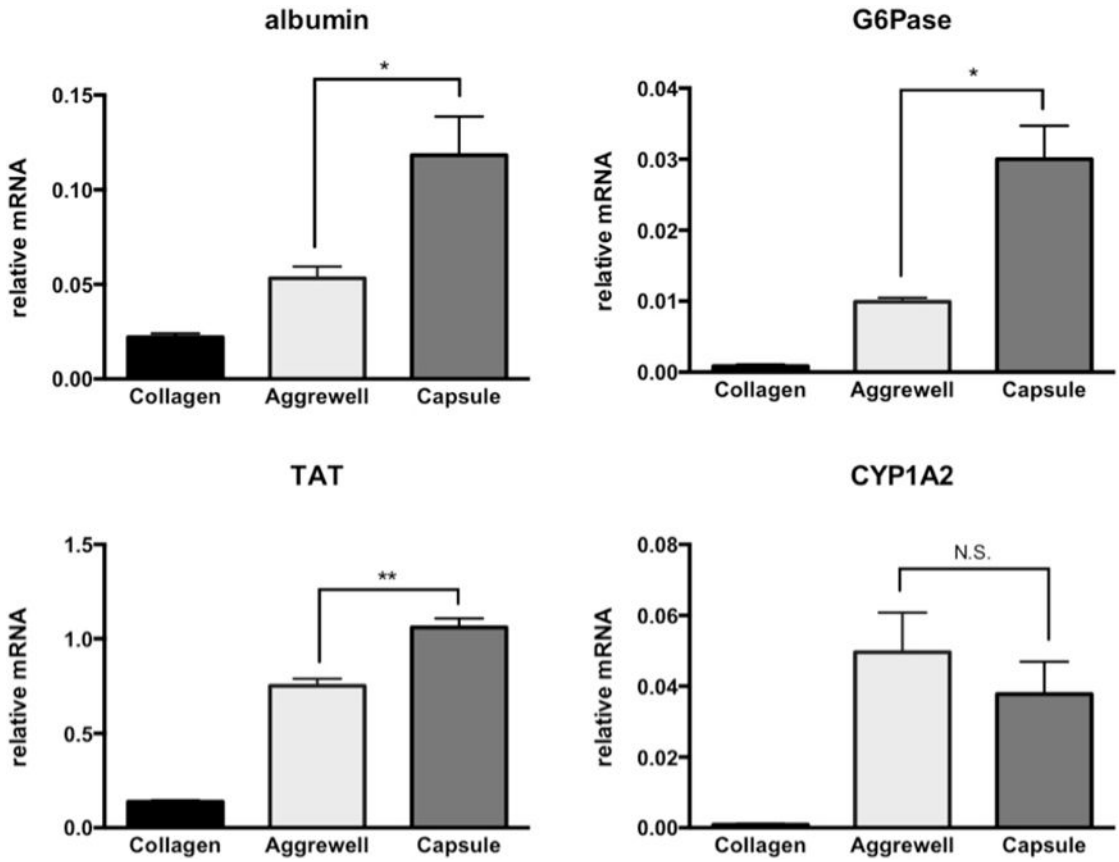

Figure 6. Analysis of hepatic gene expression

qPCR results indicate encapsulated spheroids expressed higher levels of albumin and metabolic genes (TAT and G6Pase) compared to 2D and 3D controls (Day 8). (n=3, * $p<0.05$, ** $p<0.01$)

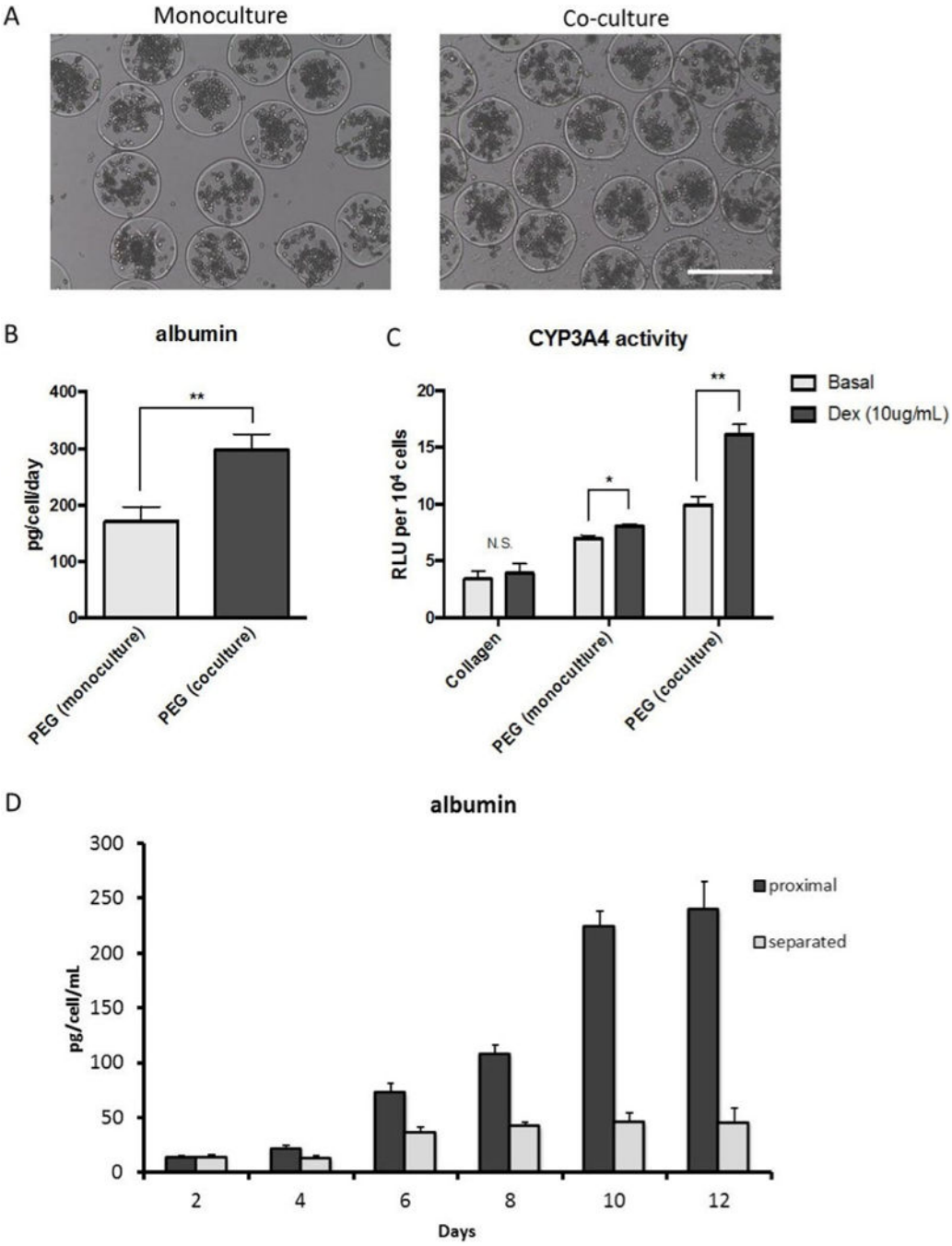

Figure 7. Co-culture of microcapsules with 3T3-J2 fibroblasts improves hepatic function

(A) For co-culture experiments, microcapsules were seeded directly onto a fibroblast monolayer, and (B-C) exhibited higher levels of albumin secretion and induced CYP3A4 activity on Day 7. (D) Albumin ELISA results for transwell cultures comparing the effects of proximity between fibroblasts and hepatocytes. (n=3, * $p<0.05$, ** $p<0.01$). Scale bar = 500 μm.